Thyrospheres From Normal or Malignant Thyroid Tissue Have Different Biological, Functional, and Genetic Features

Fiorenza Gianì,* Veronica Vella,* Maria Luisa Nicolosi, Alessandra Fierabracci, Sonia Lotta, Roberta Malaguarnera, Antonino Belfiore, Riccardo Vigneri, and Francesco Frasca

Department of Clinical and Molecular Bio-Medicine (F.G., V.V., M.L.N., S.L., R.V., F.F.), Endocrinology Unit, Garibaldi-Nesima Medical Center, University of Catania, 95122 Catania, Italy; Immunology and Pharmacotherapy Area (A.F.), Bambino Gesù Children's Hospital, Istituto di Ricovero e Cura a Carattere Scientifico, 00165 Rome, Italy; Department of Motor Sciences (V.V.), School of Human and Social Sciences, "Kore" University of Enna, 94100 Enna, Italy; Division of Endocrinology (R.M., A.B.), Department of Health Sciences, University Magna Graecia of Catanzaro, 88100 Catanzaro, Italy; and HUMANITAS (R.V.), Catania Oncology Center, 95126 Catania, Italy

Context: Cancer stem cells from several human malignancies, including poorly differentiated thyroid carcinoma and thyroid cancer cell lines, have been cultured in vitro as sphere-forming cells. These thyroid cancer stem cells were proven to be able to reproduce the original tumor in a xenograft orthotopic model.

Objectives: The objective of the study was to characterize papillary thyroid carcinoma (PTC) spheres from well-differentiated thyroid cancer and normal thyroid (NT) spheres obtained from the contralateral thyroid tissue of the same patient.

Design: Thyrospheres from PTCs and NTs were isolated.

Main Outcome Measures: Gene expression analysis by real-time PCR, immunofluorescence studies, and fluorescence-activated cell sorter analysis in thyrospheres from PTCs and NTs have been evaluated.

Conclusions: Compared with NT spheres, PTC spheres are larger, more irregular, and more clonogenic and have a higher rate of symmetric division. Moreover, PTC spheres express higher levels of stem cell markers and lower levels of thyroid-specific genes compared with NT spheres. Under appropriate conditions, NT spheres differentiated into thyrocytes, whereas PTC spheres did not, displaying a defect in the differentiation potential. Immunofluorescence experiments indicated that, in NT spheres, progenitor cells are mainly present in the sphere core, and the sphere periphery contains thyroid precursor cells already committed to differentiation. PTC spheres are not polarized like NT spheres. Unlike cells differentiated from NT spheres, TSH did not significantly stimulate cAMP production in cells differentiated from PTC spheres. A microarray analysis performed in paired samples (NT and PTC spheres from the same patient) indicated that NT and PTC spheres display a gene expression pattern typical of stem/progenitor cells; however, compared with NT spheres, PTC spheres display a unique gene expression pattern that might be involved in PTC progression. **(*J Clin Endocrinol Metab* 100: E1168–E1178, 2015)**

ISSN Print 0021-972X ISSN Online 1945-7197
Printed in USA

Received November 19, 2014. Accepted June 30, 2015.
First Published Online July 7, 2015

* F.G. and V.V. contributed equally to this work.

Abbreviations: ABCG-2, ATP-binding cassette, sub-family G, member 2; ALDH, aldehyde dehydrogenase; CFDA, carboxyfluorescein diacetate succinimidyl ester; CSC, cancer stem cell; DVL1, Dishevelled segment polarity protein 1; NT, normal thyroid; OCT-4, octamer-binding transcription factor 4; SOX-2, SRY (sex determining region Y)-box 2; PTC, papillary thyroid carcinoma; RT, reverse transcription; TCSC, thyroid cancer stem cell; TNSC, thyroid normal stem cell.

Thyroid tumors have been hypothesized to follow a classic multistep carcinogenesis model with mutations (including BRAF and RAS mutations) causing constitutive activation of the MAPK pathway, responsible for most differentiated thyroid carcinomas. Additional mutations in phosphatidylinositol 3-kinase pathway are involved in poorly differentiated thyroid carcinomas progression (1). According to this stochastic model, thyroid cancer initiation is monoclonal and acquires heterogeneity during tumor progression by additional mutations that deregulate cell proliferation, differentiation, and survival (2). This hypothesis is supported by histological observation of areas of well-differentiated thyroid cancer within poorly differentiated and anaplastic thyroid cancer specimens and vice versa (3, 4).

An alternative stem cell model has been hypothesized for thyroid cancer initiation and progression (5). According to this model, a hierarchical cancer cell organization is present; only a subset of cancer cells that could self-renew give rise to progenitor cells that drive tumor growth (6). Through uncontrolled proliferation, these undifferentiated and pluripotent cells could directly give rise to a variety of different cancers and play a major role in metastases and resistance to chemo- and radiotherapy (7). Cancer stem cells (CSCs) arise through mutations or epigenetic changes acquisition from normal adult stem cells or their committed progenitor cells (5). They have been isolated from several solid tumors including thyroid cancer (8) and are able to form spheres in vitro and to generate the original tumor when transplanted into immunodeficient mice (8).

For thyroid cancer, the stem cell hypothesis is supported by findings that several signaling pathways typical of adult stem cells (ie, the Wnt pathway, Hedgehog and Notch signaling pathways) are up-regulated in thyroid malignancies (9–11). Furthermore, there are close relationships between gene expression patterns in embryonic stem cells (such as oncofetal fibronectin and p63) (12–15) and some thyroid malignancies. However, whether thyroid cancer cells are derived from mutated adult stem cells or from their committed progenitors or whether they display a newly acquired stem-like phenotype due to cancer mutations remains controversial (7).

Adult thyroid stem cells from normal or goiter thyroid tissue and putative CSCs from thyroid cancer cell lines were recently isolated in vitro as thyrospheres (8, 16–19). In adult human thyroid specimens, stem cells and progenitor cells were detected as single cells or as groups of two or three cells throughout the tissue (20). The orthotopic injection of a few thyroid CSCs could reproduce the parental thyroid cancer (8), a prerequisite for demonstrating the tumor-forming capacity of thyroid CSCs. These data have been questioned because not all CSCs derived from thyroid carcinoma cell lines could generate tumors in a xenograft model (19). These discrepancies could be a consequence of the use of different mice strains, different sites of injections, or additional humanization procedures (use of matrigel matrix for the xenografts). In addition, stem/progenitor cells might be very heterogeneous, and their selection could be influenced by the use of different markers of stemness. Different thyroid CSC subpopulations might have different roles in tumor formation/progression.

To understand the biology of thyroid CSCs, we comparatively characterized in vitro thyrosphere forming cells derived from well-differentiated thyroid carcinomas [papillary thyroid carcinoma (PTC) spheres] and thyrospheres from the normal contralateral thyroid tissue of the same patients.

Materials and Methods

Patients, tissues, and cell lines

Surgical pathological specimens were obtained from patients aged 52–65 years affected by classic variant papillary thyroid cancer (stage I-III, tumor size 1–3 cm) (Supplemental Table 1) (21–23). Corresponding normal-appearing tissues were available with each specimen and used to establish normal thyroid primary cultures. The study was approved by the local ethics committee and all patients provided written informed consent.

Normal thyroid primary cultures from tissue specimens were established from normal thyroid tissue, as previously described (24). Cell lines used included the following: HT-29 (25) from human colon cancer (Dr A. Fusco, University of Naples, Naples, Italy) grown in RPMI 1960 medium (Sigma); HepG2 from human hepatocarcinoma (American Type Culture Collection) grown in MEM and FRTL5 cells from rat thyroid (Dr G. Damante, University of Udine, Udine, Italy) grown in Coon's modified Ham's F12 medium (as for primary cultures). All media were supplemented with glutamine, 10% fetal bovine serum, or penicillin/streptomycin or with 5% calf serum or the six-hormone mixture (for primary cultures and FRTL5).

Thyrospheroid culture

Thyrospheroids were generated as previously described (16). Briefly, single cells from tissue digestion were cultured at a density of 10 000–30 000 cells/mL in low-attachment flasks in DMEM/F12 (Sigma), B27 supplement (Life Technologies, MB), and human recombinant epidermal and basic fibroblast growth factors (20 ng/mL each).

To assess self-renewal, spheres were enzymatically dissociated and replated at a density of 50 000 cells/ml in six-well culture dishes in stem cell conditions. Secondary thyrospheres were counted at day 15, and their volume was evaluated using an Olympus optical microscope supported by a DP20–5E digital camera.

For differentiation experiments, thyrospheres were collected, enzymatically dissociated (5 min with StemPro Accutase at 37°C; Life Technologies), and seeded in petri dishes in DMEM/Ham's F-12 containing 10% fetal bovine serum at a density of 5000 cells/mL. Cells grew as monolayers, and, after 3 days, they were stimulated with TSH (5 mIU/L). At days 0 and 15, cells were harvested for gene expression analysis.

HT-29 (25) cells were used because they represent a positive control for stem cell markers and a negative control for thyroid specific markers expression.

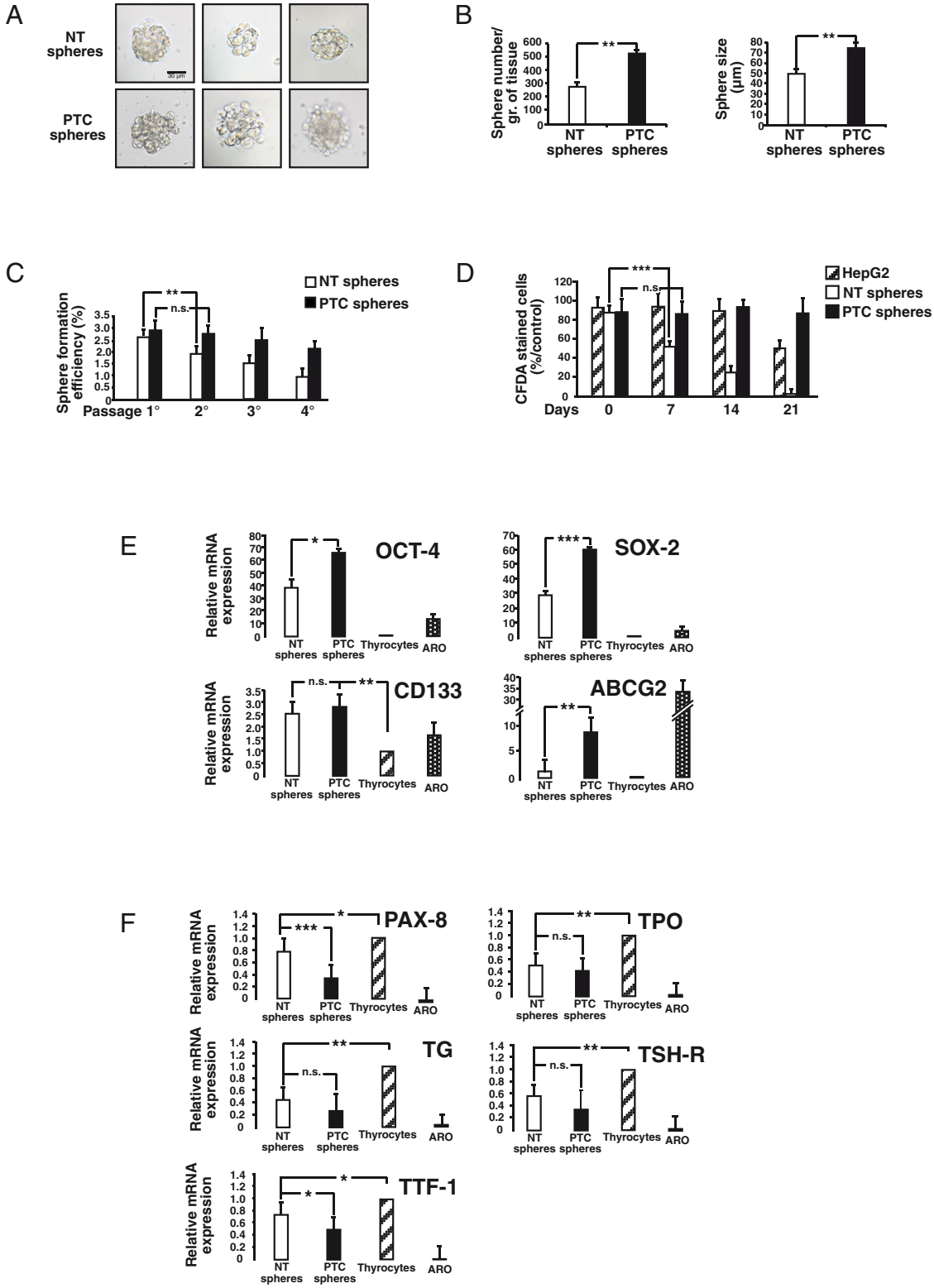

Figure 1. Phenotypic characterization of human NT and PTC spheres. A, Inverted microscope images of human NT (top) and PTC spheres (bottom) obtained 10 days after single-cell plating. Representative images are shown. B, Number of NT (white bar) and PTC spheres (black bar) obtained per gram of thyroid tissue. Values are mean ± SE from 10 separate preparations from independent patients (left panel). Each experiment was performed in triplicate. Size (micrometers) of NT (white bar) and PTC spheres (black bar). A cutoff size of 70 μm in diameter was considered for sphere countings. The numbers were obtained by scoring spheres by an inverted microscope with an integrated caliper (at least 50 spheres for each preparation) and are the mean ± SE of 10 separate preparations from independent patients (right panel). Each experiment was performed in triplicate. C, Sphere formation efficiency. Spheres were scored every 7–10 days after repeated single-cell plating. The numbers were obtained using sphere counting by an inverted microscope and are expressed as the percentage of spheres over total plated cells. NT (white bar) and PTC spheres (black bar). Values are mean ± SE of 10 separate preparations from independent patients. Each experiment was performed in triplicate. D,

Gene expression analysis

Total RNA was extracted using the PureLink RNA minikit (Invitrogen, Life Technologies, MB). cDNA was synthesized with the ThermoScript RT-PCR system for first-strand cDNA synthesis (Invitrogen, Life Technologies, MB) using oligodeoxythymidine following the manufacturer's instructions.

Real-time PCR was performed with the ABI 7500 real-time PCR system (Applied Biosystems, Life Technologies, MB) using probe, primer sets, and Taqman universal master mix (Taqman gene expression assay; Applied Biosystems, Life Technologies, MB). Human glyceraldehyde-3-phosphate dehydrogenase was used for normalization. mRNA quantification was performed using the comparative cycle threshold method (delta-deltaCt).

To perform the real-time PCR array, 1 μg of RNA was converted into cDNA using the RT^2 first-strand kit (SABiosciences, QIAGEN). One microgram of RNA was mixed with genomic DNA elimination buffer (SABiosciences, QIAGEN) and then mixed with the reverse transcription (RT) cocktail (RT buffer, primer, and control mix, RT enzyme; SABiosciences, QIAGEN) for cDNA synthesis. For each array, 102 μL cDNA and 1173 μL double-distilled H_2O were mixed with 1275 μL of the 2× RT^2 SYBR Green quantitative PCR master mix. This final mixture (25 μL) was added to each well of the human stem cell RT^2 Profiler PCR array (SABiosciences, QIAGEN; catalog number PAHS-405ZA). A two-step real-time PCR was performed, starting at 95°C (10 min) for one cycle, followed by 95°C (15 sec) and 60°C (1 min) for 40 cycles.

Relative gene quantification was evaluated using the comparative threshold cycle method. In thyrospheres, fold changes were calculated as the gene expression difference in respect to thyrocytes in primary culture (calibrator).

Five endogenous control genes, RT controls, and PCR controls were included. Eighty-four genes related to the identity, growth, and differentiation were evaluated.

Immunofluorescence studies

Spheres were plated onto poly-D-lysine-coated glass coverslips, fixed with formaldehyde (Polysciences GmbH), permeabilized with Triton X-100, and blocked with normal goat serum. The following antibodies were incubated overnight at 4°C: anti-Oct-4 (rabbit polyclonal; Cell Signaling); anti-Tg (mouse monoclonal, sc-51708; Santa Cruz Biotechnology); antivimentin (mouse monoclonal, sc-6260; Santa Cruz Biotechnology); and anticytokeratin 1/10 (mouse monoclonal, sc-53251; Santa Cruz Biotechnology). Alexa-conjugated (Alexa Fluor 594 or 488) secondary antibodies (Molecular Probes, Life Technologies) were then added for 1 hour. Alexa-conjugated phalloidin (Molecular Probes, Life Technologies) and Hoechst (Sigma) were used to visualize, respectively, cytoplasm and nuclei. Epifluorescence microscopy was performed using an Olympus microscope. Images were digitally acquired using an Orca charge-coupled device camera (Hamamatsu) and processed using Image-Pro Plus 4.0 software (Media Cybernetics).

Cell division evaluation

Cells were incubated with carboxyfluorescein diacetate succinimidyl ester (CFDA), a fluorescent dye that is retained in living cells. The fluorescence intensity decay is proportional to the extent of asymmetric division. Serial halving of the fluorescence intensity of CFDA (Molecular Probes, Life Technologies) was determined by flow cytometry immediately after staining and 7, 14, and 21 days later.

Response to TSH

Basal and TSH-stimulated cAMP was measured using the cAMP Biotrak competitive enzyme immunoassay system (Amersham, GE Healthcare Europe GmbH) based on the competition between unlabeled cAMP in the sample and a fixed quantity of peroxidase-labeled cAMP conjugate. Cells were cultured in 5-hormone medium lacking TSH for 24 hours and then stimulated for 2 hours with increasing concentrations of human TSH. cAMP extraction was performed with anti-cAMP antiserum and then immobilized onto donkey-antirabbit Ig-precoated microplates. cAMP concentration in each sample was calculated by substrate absorption measured at 450 nm and quantitatively compared with the cAMP standard curve.

Clustergram analysis and heat map graph of gene expression data

The unsupervised hierarchical cluster analysis and heat map graph were constructed using the online RT^2 Profiler PCR array software provided by SABiosciences (QIAGEN). The mRNA expression profile of the thyrospheres was represented as a heat map graph, and genes were clustered according to their expression patterns.

Scatter plot analysis of PCR array results

Thyroid cancer stem cell (TCSC) and thyroid normal stem cell (TNSC) data were plotted using the SAbiosciences (QIAGEN) web-based RT^2 Profiler PCR array data analysis tool and then exported.

Statistical analysis

Differences between the means were analyzed by a Student's test for unpaired samples. A value of $P < .05$ was considered statistically significant. Statistical analysis was carried out with GraphPad software (Prism).

Results

Phenotypic characterization of human normal thyroid (NT) and PTC spheres

When comparing an equal amount (by weight) of normal vs malignant cancer tissue, we observed that thyroid cancer tissue provided a greater number of thyrospheres

Figure 1 (Continued). Cell division rate in spheres from normal (NT, white bars) and malignant (PTC, black bars) thyroid tissue. HepG2 spheres (hatched bars) were used as a control. Fluorescence-activated cell sorter analysis was performed at the indicated time points after CFDA staining (see *Materials and Methods*). The numbers are expressed as the percentage of control and are the mean ± SE of 12 separate preparations from independent patients. Each experiment was performed in triplicate. E, Stem cell markers in NT (white bars) and PTC spheres (black bars) after 7 days of culture and in normal thyrocytes (hatched bars) and HT-29 cells (dotted bars) used as controls. The values indicate fold changes over normal thyrocytes used as a calibrator and are the mean ± SE of 16 separate preparations from independent patients. Each experiment was performed in triplicate. F, Thyroid-specific markers in NT (white bars) and PTC spheres (black bars) after 7 days of culture and in normal thyrocytes (hatched bars) and HT-29 cells (dotted bars). The values indicate fold changes over normal thyrocytes used as a calibrator and are the mean ± SE of 16 separate preparations from independent patients. Each experiment was performed in triplicate. N.S., nonsignificant difference. *, $P < .05$; **, $P < .01$; ***, $P < .001$.

(Figure 1B, left panel); this result could be a possible consequence of either the increased clonogenic potential of malignant stem cells or a higher absolute stem cell number or the overall cell number increase due to increased cell density in cancer tissue compared with the colloid-replenished follicles of normal thyroid tissue. The sphere-forming ability was evaluated in *BRAF* mutant and wild-type PTCs. We observed a higher sphere efficiency formation in PTCs harboring the *V600E BRAF* mutation as shown in Supplemental Figure 1. The PTC spheres were also signif-

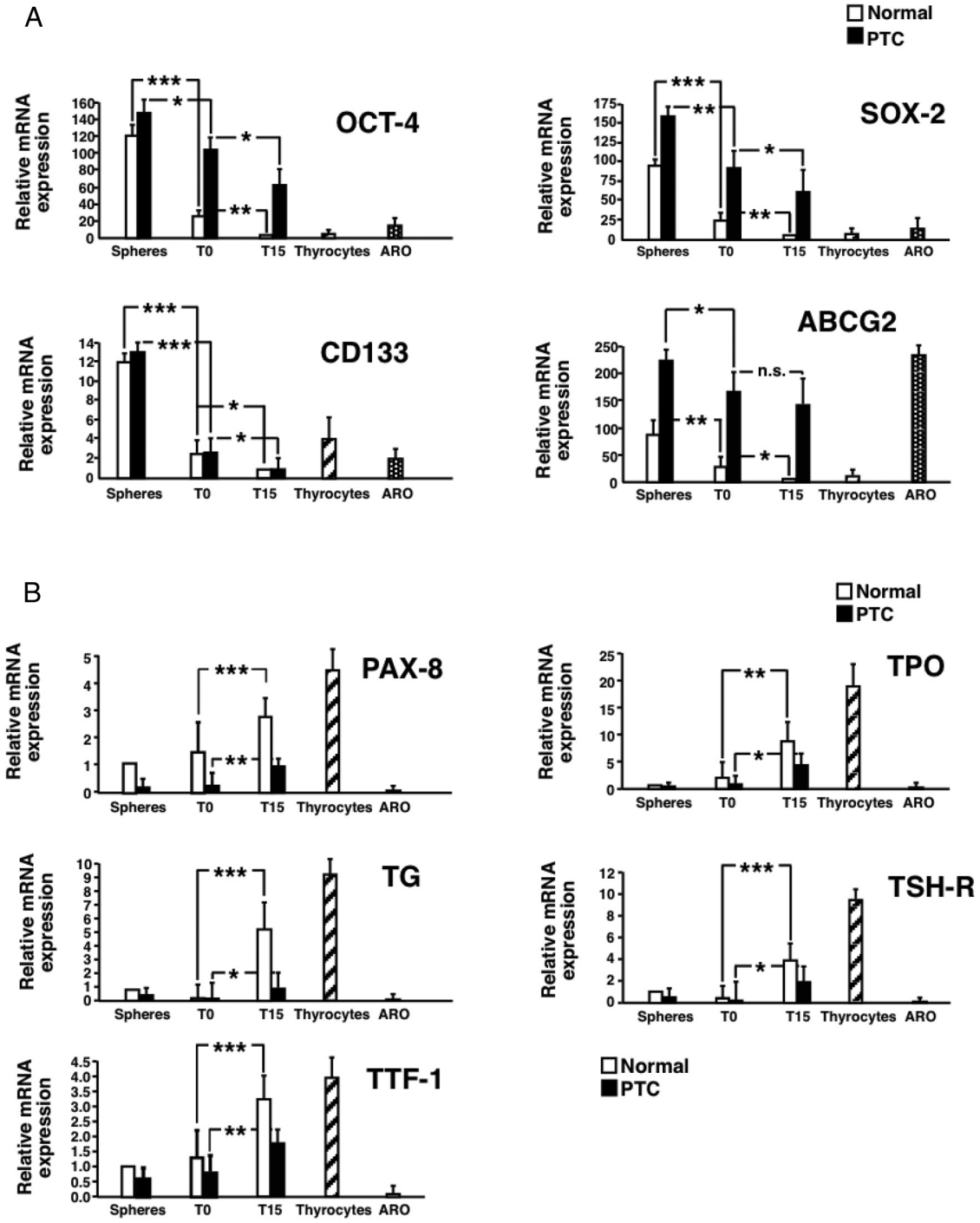

Figure 2. Expression profile of stem cell and thyroid-specific markers in NT and PTC spheres under differentiating conditions. Thyrospheres were allowed to attach (T0) and then subjected to the differentiation protocol for 2 weeks (T15), as described in *Materials and Methods*. Stem cell markers (A) and thyroid-specific markers (B) are shown in NT (white bars) and PTC spheres (black bars) and in derived differentiating cells. Normal thyrocytes in primary culture (hatched bars) and HT-29 cells (dotted bars) were used as controls. The data indicate fold changes relative to normal thyrocyte in primary culture mRNA expression used as a calibrator. Values are the mean ± SE of 18 separate preparations from independent patients. Each experiment was performed in triplicate. N.S., nonsignificant difference. *, $P < .05$; **, $P < .01$; ***, $P < .001$.

icantly larger than the NT spheres (Figure 1B, right panel) and displayed a more irregular shape (Figure 1A). When the NT and PTC spheres were dissociated to single-cell suspensions and cultured for several passages, the cells from the PTC spheres maintained a higher rate of sphere formation than the NT spheres (Figure 1C), suggesting a higher clonogenic potential of cancer progenitor cells. This difference increased with the number of passages.

To further investigate the replication potential of PTC spheres, cell division was evaluated using CFDA staining by fluorescence-activated cell sorter analysis, as described in *Materials and Methods* (Figure 1D). HepG2 cells were used as a control for CFDA decay (Figure 1D). PTC spheres retained CFDA at a higher extent than NT spheres, with a significant difference present as early as day 7 and increasing thereafter. These data suggest a higher rate of symmetric division in PTC-derived spheres (Figure 1D).

These results indicate that, compared with the NT spheres, PTC spheres are more numerous, larger, more irregular, and more clonogenic and have a higher rate of symmetric division.

Stem cell marker expression was evaluated using quantitative RT-PCR in NT and PTC spheres (n = 5). Primary thyrocytes and HT-29 (25) cells were used as controls. Octamer-binding transcription factor 4 (*OCT-4*), SRY (sex determining region Y)-box 2 (*SOX-2*), *CD133*, and ATP-binding cassette, sub-family G, member 2 (*ABCG-2*) expression levels were significantly higher in thyrospheres than in thyrocytes in primary culture (Figure 1E). *OCT-4, SOX-2*, and *ABCG-2* expression, but not *CD133* expression, was significantly increased in PTC compared with NT spheres (Figure 1E). The expression of thyroid-specific genes *PAX-8*, thyroperoxidase (*TPO*), thyroglobulin (*Tg*), TSH receptor (*TSH-R*), and *TTF-1* was significantly lower in thyrospheres compared with a pool of four preparations of normal thyrocytes in primary culture (Figure 1F). The expression of *PAX-8* and *TTF-1* was significantly lower in PTC spheres than in NT spheres (Figure 1F). All of these markers were undetectable in HT-29 cells (Figure 1F).

These results indicate that thyrospheres express higher levels of stem cell markers than normal thyrocytes in primary culture; however, thyrospheres express a lower level of thyroid specific genes. Moreover, PTC spheres express higher levels of stem cell markers and lower levels of thyroid-specific gene markers compared with NT spheres.

PTC spheres have a lower differentiation potential than NT spheres

Previous reports indicate that, under proper conditions, human thyrospheres might differentiate into thyrocytes (16, 17). We evaluated the changes in stem and thyroid-specific genes expression in NT and PTC spheres during the differentiation procedure (Figure 2). The expression of the stem cell markers *OCT-4, SOX-2, CD133*, and *ABCG-2* significantly decreased in NT and PTC spheres incubated under differentiation conditions (Figure 2A, T0) and further decreased in sphere-derived cells after 15 days (T15, Figure 2A). The decrease in *OCT-4, SOX-2*, and *ABCG2* was significantly greater in NT than in PTC spheres (Figure 2A), reaching values as low as those observed in normal thyrocytes in primary culture (Figure 2A).

Thyroid-specific genes *PAX-8*, *TPO*, TG, *TSH-R*, and *TTF-1* progressively increased during differentiation (Figure 2B). The increase was lower in PTC spheres compared with NT spheres (Figure 2B). However, values observed in

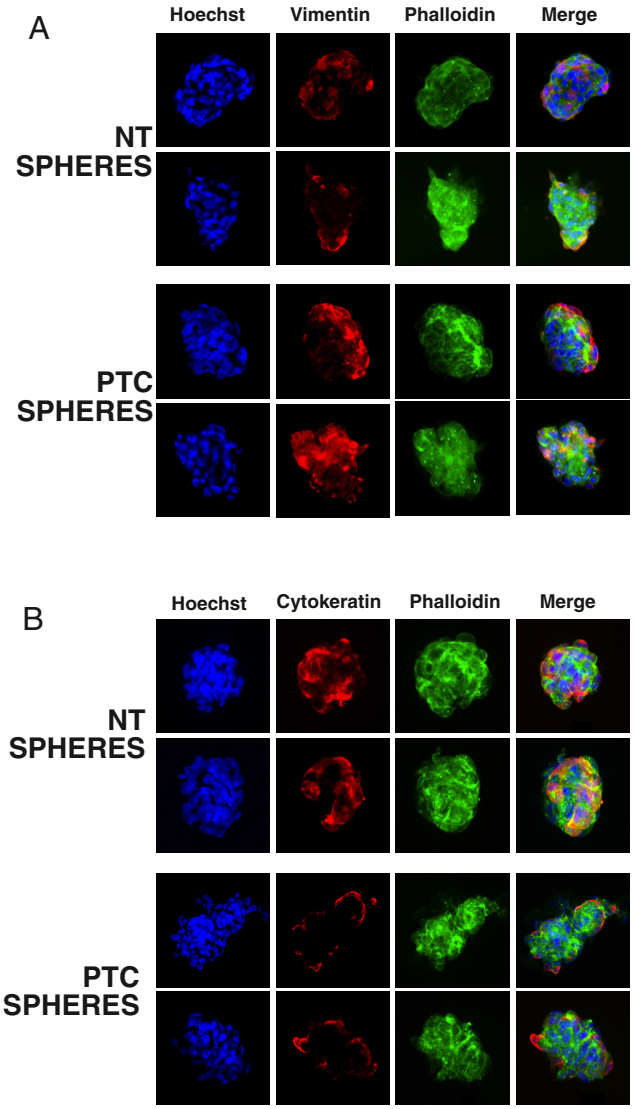

Figure 3. Mesenchymal and epithelial markers in NT and PTC spheres. Thyrospheres were plated onto poly-D-lysine-coated glass coverslips and subjected to immunofluorescence, as described in *Materials and Methods*. Staining with antivimentin antibody (green; A) and anticytokeratin antibody (green; B) in NT (upper panels) and PTC spheres (lower panels). The nuclei were counterstained with Hoechst (blue), and the cytoplasm was stained with phalloidin (red).

NT spheres at day 15 (T15, Figure 2B) remained lower than in thyrocytes in primary culture.

These data suggest that, under proper conditions, NT spheres differentiate into thyrocytes, whereas PTC spheres display a defective differentiation potential.

Thyrospheres express epithelial and mesenchymal markers and are polarized

We further explored thyrosphere phenotype by immunofluorescence (Figure 3). Cytokeratin staining was stronger in the NT spheres, whereas vimentin staining was stronger in the PTC spheres (Figure 3, compare panel A with panel B). Moreover, by Western blot analysis, we found a reduced expression of E-cadherin in TCSCs compared with TNSCs (Supplemental Figure 2).

These data suggest that PTC spheres might be more susceptible to epithelial-mesenchymal transition than NT spheres, as previously reported in human cancer mammospheres (26).

To evaluate the cell distribution related to differentiation within the single sphere, we performed immunoflu-

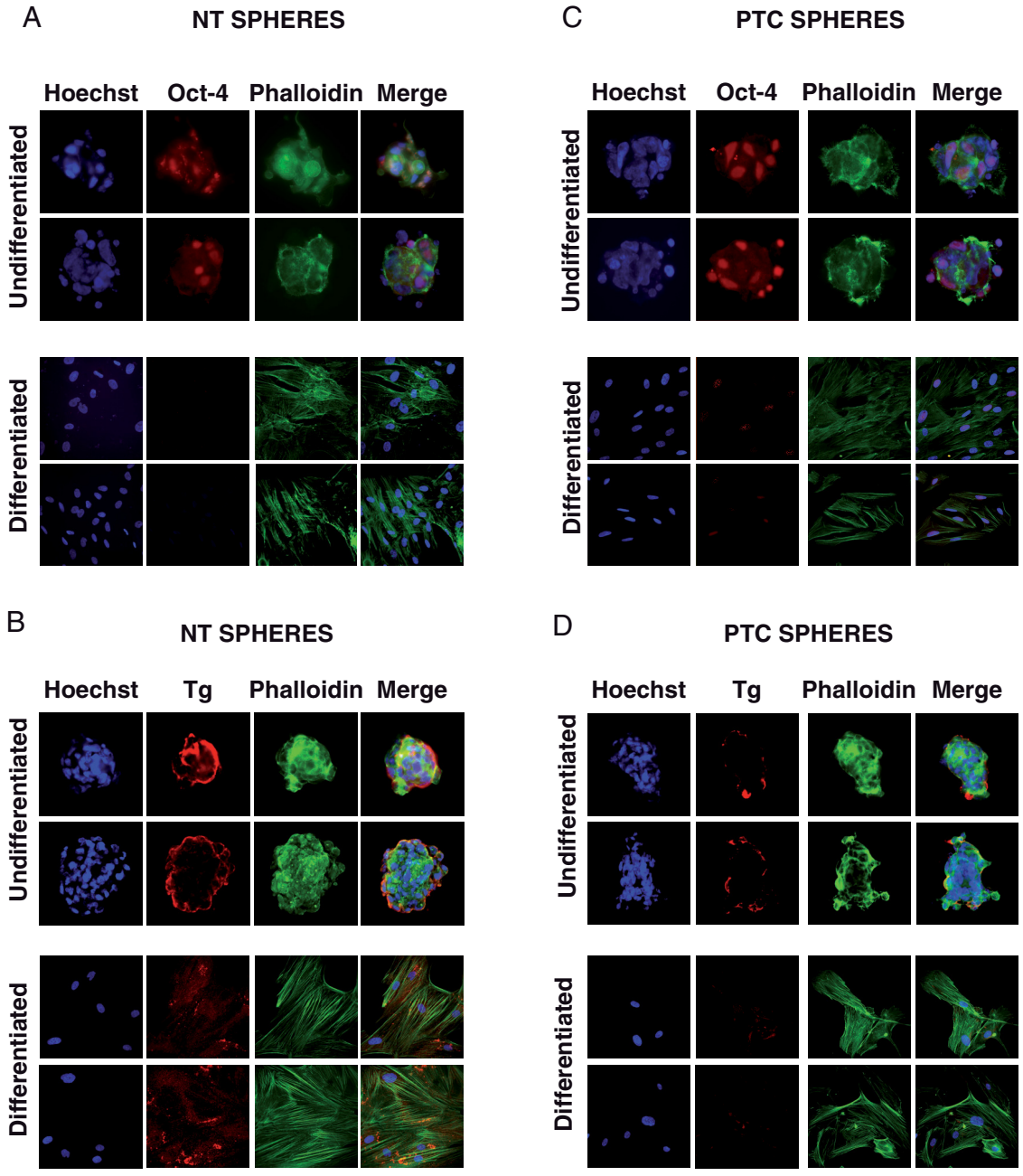

Figure 4. Immunofluorescence for stem cell and thyroid-specific markers in NT (A) and PTC (B) spheres. Thyrospheres were plated onto poly-D-lysine-coated glass coverslips and subjected to immunofluorescence, as indicated in *Materials and Methods*. A, Upper panel, Staining with anti-OCT4 antibody (red) in NT and PTC spheres. The nuclei were counterstained with Hoechst (blue), and the cytoplasm was stained with phalloidin (green). B, Lower panel, Staining with antithyroglobulin antibody (red) in NT and PTC spheres. The nuclei were counterstained with Hoechst (blue), and the cytoplasm was stained with phalloidin (green).

orescence experiments using anti-*OCT-4* (stemness marker) and antithyroglobulin (differentiated marker) antibodies (Figure 4). In NT spheres, *OCT-4* staining was clearly more intense in the core than in the sphere periphery (Figure 4A); in PTC spheres, the staining was more scattered (Figure 4C). In contrast, thyroglobulin staining was detected mainly at NT sphere periphery (Figure 4B) and was very weak in PTC spheres (Figure 4D).

These results indicate that more undifferentiated progenitors are mainly present in the sphere core of NT spheres, whereas cells already committed to differentiation are mainly located in the sphere periphery. In contrast, PTC spheres are less susceptible to differentiation and are not architecturally organized like NT spheres.

NT and PTC sphere-derived cell response to TSH stimulation

To evaluate the differentiation ability, spheres were stimulated with increasing doses of TSH. c-AMP production was measured as described in *Materials and Methods*. In differentiated cells from the NT spheres, TSH stimulated cAMP production in a dose-dependent manner with a maximal increase of approximately 10-fold at 100 nM TSH, following a pattern similar to that observed in FRTL-5 cells and in human thyrocytes in primary culture (Figure 5). In contrast, TSH weakly stimulated cAMP production in differentiated cells from the PTC spheres. These results confirm that PTC spheres have a lower capacity to differentiate compared with NT spheres, which is consistent with the previously described morphological and functional parameters.

PTC spheres express a distinct gene pattern

Gene expression pattern was studied in paired samples of TNSCs and TCSCs obtained from the same patient. A pool of four preparations of normal thyrocytes in primary culture was used as reference. Compared with normal thyrocytes in primary culture, normal thyrospheres displayed the up-regulation of several genes, including cell cycle regulator *APC*, cell-cell communication gene *DLL1*, and the WNT pathway gene *FRAT-1* (Figure 6A). All these genes were up-regulated by severalfold in spheres. Compared with normal thyrocytes, normal thyrospheres displayed a consistent down-regulation of the *CDK1* and *BMP2* genes (Figure 6A). Moreover, important differences in gene expression were observed between NT and PTC spheres. *DLL1*, *GJB2*, *ABCG2*, *DVL1*, *WNT1*, and *KRT15* were selectively up-regulated in PTC vs NT spheres (Figure 6B). Several other genes, including *APC*, *IGF1*, *NCAM1*, and *ALDH1A1* (Figure 6B), were selectively up-regulated in NT spheres. These results indicate that NT and PTC spheres display a gene expression pattern typical of stem/progenitor cells; however, compared with the NT spheres, the PTC spheres display a unique gene expression pattern.

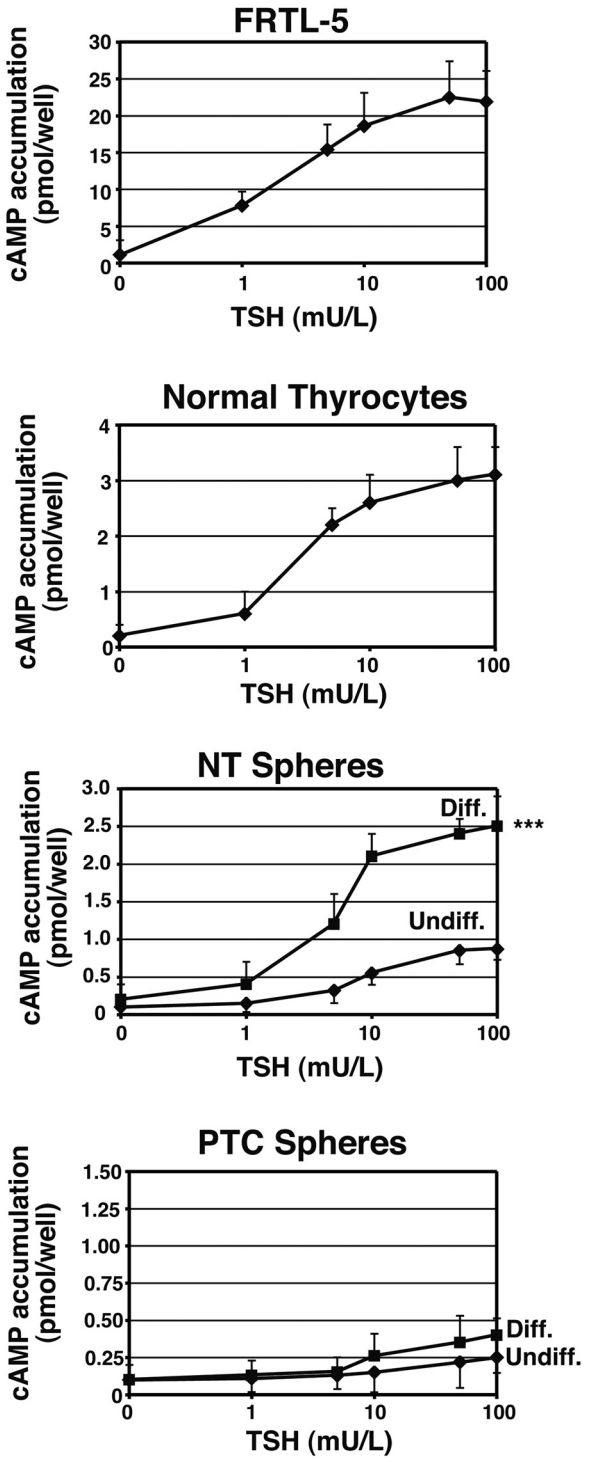

Figure 5. cAMP production in response to TSH in undifferentiated or differentiated NT and PTC spheres. Thyrospheres were subjected to the differentiation protocol or not subjected to the protocol. The thyrospheres were then stimulated with increasing doses of TSH, and the cAMP was measured as described in *Materials and Methods*. Rat FRTL-5 and normal human thyrocytes in primary culture were used as positive controls. Pooled cells from eight preparations of NT and PTC spheres were used. The data indicate the mean ± SE of four separate experiments performed in triplicate. *, $P < .05$; **, $P < .01$; ***, $P < .001$.

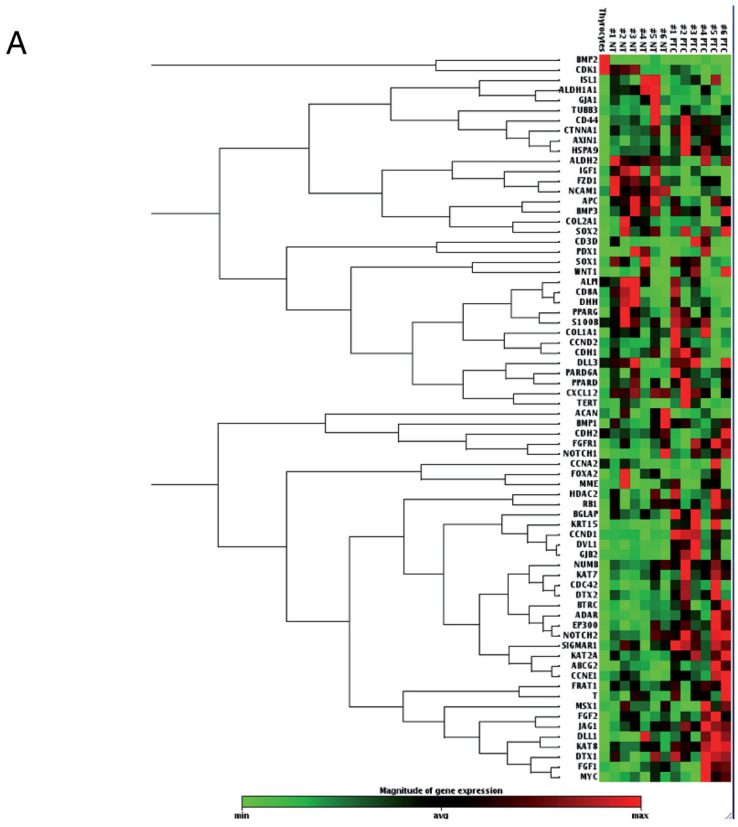

	Gene	TCSCs	TNSCs	Fold Regulation
Genes Over-Expressed in CSCs vs TNSCs	ABCG2	0.000239	0.000029	8,35
	ADAR	0.024565	0.008938	2,75
	BTRC	0.001194	0.000344	3,48
	CCND1	0.098099	0.027409	3,58
	CCNE1	0.003883	0.001866	2,08
	CDC42	0.118750	0.054505	2,18
	DLL1	0.000848	0.000118	7,15
	DTX2	0.008241	0.003626	2,27
	FYL1	0.066748	0.022059	3,03
	EP300	0.013117	0.005167	2,54
	KAT2A	0.017999	0.007491	2,40
	GJB2	0.010553	0.001516	6,96
	HDAC2	0.000077	0.000035	2,18
	KRT15	0.001975	0.000349	5,65
	KAT8	0.017610	0.008569	2,06
	KAT7	0.013766	0.006286	2,19
	PARD6A	0.001328	0.000407	3,27
	TERT	0.000089	0.000025	3,53
	WNT1	0.000013	0.000002	6,94
Genes Down-Expressed in CSCs vs TNSCs	ACAN	0.000016	0.000055	-3,34
	ALDH1A1	0.001656	0.004731	-2,86
	ALP1	0.000008	0.000017	-2,17
	APC	0.000084	0.000266	-3,15
	BMP2	0.001464	0.003380	-2,31
	CDK1	0.000822	0.002190	-2,66
	CDH2	0.001590	0.003912	-2,46
	COL2A1	0.000010	0.000049	-5,18
	CXCL12	0.006185	0.013224	-2,14
	FZD1	0.012680	0.031626	-2,49
	GJA1	0.003973	0.070485	-2,41
	IGF1	0.000101	0.003266	-32,41
	PDX1	0.000006	0.000017	-2,84
	NCAM1	0.000290	0.007260	-25,03

Figure 6. Clustergram analysis, heat map graph of gene expression data (A), and scatter plot analysis of PCR array (B). A, The mRNA expression profile of NT or PTC spheres from the same patient is shown as a heat map graph. The genes were clustered according to their expression patterns. The numbers are represented as a bitmap and are expressed as fold changes with respect to the expression profile of a pool (n = 4) of normal thyrocytes in primary culture. B, Scatter plot analysis of PCR array results from NT and PTC spheres. Each dot represents a single gene, and the boundary value was assigned as 2-fold. Up-regulation is indicated by the red dots, and down-regulation is indicated by the green dots. The scatter graph depicts a log transformation plot of the relative expression level of each gene (2-DCt) between TNSCs (x-axis) and TCSCs (y-axis). The gray lines indicate a 2-fold change in the gene expression threshold.

Discussion

The present study confirms that thyrospheres, aggregates of stem cells, and thyrocyte precursors can be isolated from normal and malignant human thyroid tissues (8, 16, 17). Under differentiation conditions, they can acquire biological and molecular characteristics similar to human thyrocytes in primary culture (16, 17).

Unlike previous studies, we compared spheres from normal and tumor thyroid tissue of the same individuals, which facilitated a better characterization of the abnormalities produced by the malignant transformation. We demonstrate that thyroid CSCs have a number of phenotypic and genotypic differences compared with the paired cells obtained from normal tissue of the contralateral thyroid lobe. These differences are morphological (PTC spheres are larger and have a less regular shape), biological (PTC spheres have a lower differentiation potential), and functional (less adherence, higher clonogenic potential, and a higher rate of symmetric division in PTC spheres) and reflect the molecular differences between thyrospheres from PTC or NT. Stemness markers, such as *OCT-4*, *SOX-2*, and *ABCG-2*, had significantly higher expression in PTC spheres, whereas thyroid-specific markers such as *TTF-1* and *PAX-8* were significantly more expressed in NT spheres, although the expression level did not reach that of mature thyrocytes in primary culture. Differences in stemness and thyroid-specific marker expression between PTC and NT spheres persist after the differentiation protocol. Thyrocytes derived from PTC spheres had a lower decrease in stemness markers and a lower increase in thyroid-specific markers. As a consequence of reduced differentiation, thyrocytes obtained from PTC spheres have a significantly reduced capacity to respond to TSH stimulation in terms of cAMP production.

Moreover, NT spheres show an organized structure with more undifferentiated cells (with high expression of stemness markers) in the cell core and precursors more committed to thyrocyte differentiation in the sphere periphery. This polarization of the sphere structure is not

evident in the PTC spheres that maintain a higher expression of the mesenchymal marker vimentin. This observation suggests that the PTC-derived spheres have an epithelial-to-mesenchymal transition feature, a marker of malignant dedifferentiation and potential cancer invasiveness.

Thyrospheres have a different gene expression pattern compared with normal thyrocytes in primary culture. In particular, *APC*, *DLL1*, and *FRAT*-1 are up-regulated in thyrospheres (Figure 6A). *APC* and *FRAT-1* are mediators of the Wnt signaling pathway (27, 28), whereas *DLL1* is a ligand of Notch signaling (29). Both pathways are involved in the maintenance of the stem cell phenotype. Moreover, thyrospheres display a consistent down-regulation of the *CDK1* and *BMP2* genes (Figure 6A). CDK1 is involved in the G2M checkpoint, which is a critical step in genome splitting into daughter cells (30); bone morphogenetic protein-2 is a TGFβ family ligand involved in cell differentiation (31). These data suggest that stemness genes are up-regulated in thyrospheres, which is consistent with their undifferentiated state.

Differences in gene expression are present in spheres obtained from malignant PTC tissue relative to normal thyroid tissue of the same individual. In particular, in PTC spheres, *DLL1*, *GJB2*, *ABCG2*, *DVL1*, *WNT1*, and *KRT15* were selectively up-regulated (Figure 6B). Several of these genes encode proteins involved in undifferentiated (cancer stem cell) phenotype maintenance and tumor aggressiveness. ABCG2 is an efflux transporter responsible for tumor chemoresistance (32). Dishevelled segment polarity protein 1 (*DVL1*) is a member of the Wnt signaling pathway, which was previously reported to be up-regulated in colon cancer in which it might play a role in tumor progression (33). DVL1 up-regulation is coincident with the up-regulation of Wnt1 that is overexpressed in several malignancies (34). Gap junction-β2 protein is a component of GTPase-activating protein junctions and might play an important role in lymph node metastases. Its up-regulation is accompanied by the epithelial-to-mesenchymal transition (35), and in PTC spheres, it is coincident with an increased expression of keratin 15, type 2, a marker of epithelial stem cells (36).

Other genes, including *APC*, *IGF1*, *NCAM1*, and *ALDH1A1* (Figure 6B), are highly expressed in the NT spheres compared with the PTC spheres. IGF-1 up-regulation is in accordance with a previous report (18) and suggests that IGF-1 might play a role in sphere differentiation. Unlike a previous report (8), we determined that *ALDH1A1* transcript levels are higher in NT spheres. These contrasting data might be explained by the possible expression of different aldehyde dehydrogenase (ALDH) isoforms in CSCs. ALDH activity, evaluated in CSCs by the Aldefluor assay, does not correlate with the *ALDH1A1* expression levels. Its activity correlates with the expression level of different isoforms (37). Because *ALDH1A1* is involved in retinoic acid synthesis and retinoic acid is an important differentiation factor (38), NT sphere *ALDH1A1* expression could be important for progenitor cell differentiation.

These data indicate that there is a general thyrosphere signature based on the expression of stem markers and up-regulation of Wnt signaling, a gene profile involved in stem phenotype and commitment to differentiation. Our molecular analysis suggests a PTC sphere signature based on the up-regulation of Wnt and Notch signaling, and epithelial-mesenchymal transition and chemoresistance enhancement. However, the specific role of these pathways in PTC spheres and in thyroid tumor progression requires additional studies.

Acknowledgments

Address all correspondence and requests for reprints to: Riccardo Vigneri, MD, Endocrinology Unit, Department of Clinical and Molecular Bio-Medicine, University of Catania, Garibaldi-Nesima Medical Center, Via Palermo 636, 95122 Catania, Italy. E-mail: vigneri@unict.it.

This work was partially supported by a grant from the Associazione Italiana Ricerca Sul Cancro and the Ministry of Education, Universities, and Research (to R.V.) and from Associazione Italiana Ricerca Sul Cancro Investigator Grant 14066/14 (to A.B.) and from Ministero della Salute Grant 67/GR-2010–2319511 (to R.M.).

Disclosure Summary: The authors have nothing to disclose.

References

1. **Nikiforov YE, Nikiforova MN.** Molecular genetics and diagnosis of thyroid cancer. *Nat Rev Endocrinol*. 2011;7:569–580.
2. **Parameswaran R, Brooks S, Sadler GP.** Molecular pathogenesis of follicular cell derived thyroid cancers. *Int J Surg*. 2010;8:186–193.
3. **McIver B, Hay ID, Giuffrida DF, et al.** Anaplastic thyroid carcinoma: a 50-year experience at a single institution. *Surgery*. 2001; 130:1028–1034.
4. **Venkatesh YS, Ordonez NG, Schultz PN, Hickey RC, Goepfert H, Samaan NA.** Anaplastic carcinoma of the thyroid. A clinicopathologic study of 121 cases. *Cancer*. 1990;66:321–330.
5. **Dick JE.** Stem cell concepts renew cancer research. *Blood*. 2008; 112:4793–4807.
6. **Rasheed ZA, Kowalski J, Smith BD, Matsui W.** Concise review: emerging concepts in clinical targeting of cancer stem cells. *Stem Cells*. 2011;29:883–887.
7. **Derwahl M.** Linking stem cells to thyroid cancer. *J Clin Endocrinol Metab*. 2011;96:610–613.
8. **Todaro M, Iovino F, Eterno V, et al.** Tumorigenic and metastatic activity of human thyroid cancer stem cells. *Cancer Res*. 2010;70: 8874–8885.
9. **Espada J, Calvo MB, Diaz-Prado S, Medina V.** Wnt signalling and cancer stem cells. *Clin Transl Oncol*. 2009;11:411–427.

10. **Jiang J, Hui CC.** Hedgehog signaling in development and cancer. *Dev Cell*. 2008;15:801–812.
11. **Koch U, Radtke F.** Notch and cancer: a double-edged sword. *Cell Mol Life Sci*. 2007;64:2746–2762.
12. **Higashiyama T, Takano T, Matsuzuka F, et al.** Measurement of the expression of oncofetal fibronectin mRNA in thyroid carcinomas by competitive reverse transcription-polymerase chain reaction. *Thyroid*. 1999;9:235–240.
13. **Malaguarnera R, Mandarino A, Mazzon E, et al.** The p53-homologue p63 may promote thyroid cancer progression. *Endocr Relat Cancer*. 2005;12:953–971.
14. **Malaguarnera R, Vella V, Vigneri R, Frasca F.** p53 family proteins in thyroid cancer. *Endocr Relat Cancer*. 2007;14:43–60.
15. **Takano T, Ito Y, Matsuzuka F, et al.** Expression of oncofetal fibronectin mRNA in thyroid anaplastic carcinoma. *Jpn J Clin Oncol*. 2007;37:647–651.
16. **Fierabracci A, Puglisi MA, Giuliani L, Mattarocci S, Gallinella-Muzi M.** Identification of an adult stem/progenitor cell-like population in the human thyroid. *J Endocrinol*. 2008;198:471–487.
17. **Lan L, Cui D, Nowka K, Derwahl M.** Stem cells derived from goiters in adults form spheres in response to intense growth stimulation and require thyrotropin for differentiation into thyrocytes. *J Clin Endocrinol Metab*. 2007;92:3681–3688.
18. **Malaguarnera R, Frasca F, Garozzo A, et al.** Insulin receptor isoforms and insulin-like growth factor receptor in human follicular cell precursors from papillary thyroid cancer and normal thyroid. *J Clin Endocrinol Metab*. 2011;96:766–774.
19. **Mitsutake N, Iwao A, Nagai K, et al.** Characterization of side population in thyroid cancer cell lines: cancer stem-like cells are enriched partly but not exclusively. *Endocrinology*. 2007;148:1797–1803.
20. **Thomas T, Nowka K, Lan L, Derwahl M.** Expression of endoderm stem cell markers: evidence for the presence of adult stem cells in human thyroid glands. *Thyroid*. 2006;16:537–544.
21. **Kakudo K, Bai Y, Liu Z, Ozaki T.** Encapsulated papillary thyroid carcinoma, follicular variant: a misnomer. *Pathol Int*. 2012;62:155–160.
22. **Akslen LA, LiVolsi VA.** Prognostic significance of histologic grading compared with subclassification of papillary thyroid carcinoma. *Cancer*. 2000;88:1902–1908.
23. **Cancer Genome Atlas Research Network.** Integrated genomic characterization of papillary thyroid carcinoma. Cell 2014;159:676–690.
24. **Milazzo G, La Rosa GL, Catalfamo R, Vigneri R, Belfiore A.** Effect of TSH in human thyroid cells: evidence for both mitogenic and antimitogenic effects. *J Cell Biochem*. 1992;49:231–238.
25. **Schweppe RE, Klopper JP, Korch C, et al.** Deoxyribonucleic acid profiling analysis of 40 human thyroid cancer cell lines reveals cross-contamination resulting in cell line redundancy and misidentification. *J Clin Endocrinol Metab*. 2008;93:4331–4341.
26. **Mani SA, Guo W, Liao MJ, et al.** The epithelial-mesenchymal transition generates cells with properties of stem cells. *Cell*. 2008;133:704–715.
27. **Gupta A, Verma A, Mishra AK, Wadhwa G, Sharma SK, Jain CK.** The Wnt pathway: emerging anticancer strategies. *Recent Pat Endocr Metab Immune Drug Discov*. 2013;7:138–147.
28. **Katoh M.** WNT signaling pathway and stem cell signaling network. *Clin Cancer Res*. 2007;13:4042–4045.
29. **Falix FA, Aronson DC, Lamers WH, Gaemers IC.** Possible roles of DLK1 in the Notch pathway during development and disease. *Biochim Biophys Acta*. 2012;1822:988–995.
30. **Malumbres M, Barbacid M.** Cell cycle, CDKs and cancer: a changing paradigm. *Nat Rev Cancer*. 2009;9:153–166.
31. **McCormack N, O'Dea S.** Regulation of epithelial to mesenchymal transition by bone morphogenetic proteins. *Cell Signal*. 2013;25:2856–2862.
32. **Gottschling S, Schnabel PA, Herth FJ, Herpel E.** Are we missing the target? Cancer stem cells and drug resistance in non-small cell lung cancer. *Cancer Genomics Proteomics*. 2012;9:275–286.
33. **Katoh M.** WNT/PCP signaling pathway and human cancer (review). *Oncol Rep*. 2005;14:1583–1588.
34. **Anastas JN, Moon RT.** WNT signalling pathways as therapeutic targets in cancer. *Nat Rev Cancer*. 2013;13:11–26.
35. **Li X, Su Y, Pan J, et al.** Connexin 26 is down-regulated by KDM5B in the progression of bladder cancer. *Int J Mol Sci*. 2013;14:7866–7879.
36. **Waseem A, Dogan B, Tidman N, et al.** Keratin 15 expression in stratified epithelia: downregulation in activated keratinocytes. *J Invest Dermatol*. 1999;112:362–369.
37. **Marcato P, Dean CA, Giacomantonio CA, Lee PW.** Aldehyde dehydrogenase: its role as a cancer stem cell marker comes down to the specific isoform. *Cell Cycle*. 2011;10:1378–1384.
38. **Simon D, Kohrle J, Schmutzler C, Mainz K, Reiners C, Roher HD.** Redifferentiation therapy of differentiated thyroid carcinoma with retinoic acid: basics and first clinical results. *Exp Clin Endocrinol Diabetes*. 1996;104(suppl 4):13–15.